



# Estimation of the direct and indirect impacts of fireworks on the physicochemical characteristics of atmospheric PM<sub>10</sub> and PM<sub>2.5</sub>

Y. Z. Tian, J. Wang, X. Peng, G. L. Shi, and Y. C. Feng

State Environmental Protection Key Laboratory of Urban Ambient Air Particulate Matter Pollution Prevention and Control, College of Environmental Science and Engineering, Nankai University, Tianjin, 300071, China

Correspondence to: G. L. Shi (nksgl@hotmail.com)

Received: 26 February 2014 – Published in Atmos. Chem. Phys. Discuss.: 6 May 2014

Revised: 1 August 2014 – Accepted: 1 August 2014 – Published: 16 September 2014

**Abstract.** To quantify the total, direct and indirect impacts of fireworks individually, size-resolved PM samples were collected before, during and after a Chinese folk festival (Chinese New Year) in a megacity in China. Through chemical analysis and morphological characterisation, a strong influence of fireworks on the physicochemical characteristics of PM<sub>10</sub> and PM<sub>2.5</sub> was observed. The concentrations of many species exhibited an increasing trend during the heavy-firework period, especially for K<sup>+</sup>, Mg<sup>2+</sup> and Cr; the results of the non-sea-salt ions demonstrated an anthropogenic influence on K<sup>+</sup> and Mg<sup>2+</sup>. Then, source apportionment was conducted by receptor models and peak analysis (PA). The total influence of the fireworks was quantified by positive matrix factorisation (PMF), showing that the fireworks contributed higher fractions (23.40 % for PM<sub>10</sub> and 29.66 % for PM<sub>2.5</sub>) during the heavy-firework period than during the light-firework period (4.28 % for PM<sub>10</sub> and 7.18 % for PM<sub>2.5</sub>). The profiles of the total fireworks obtained by two independent methods (PMF and peak analysis) were consistent, with higher abundances of K<sup>+</sup>, Al, Si, Ca and organic carbon (OC). Finally, the individual contributions of the direct and indirect impacts of fireworks were quantified by chemical mass balance (CMB). The percentage contributions of resuspended dust, biomass combustion and direct fireworks were 36.8 ± 8.37 %, 14.1 ± 2.82 % and 44.4 ± 8.26 %, respectively, for PM<sub>10</sub> and 34.9 ± 4.19 %, 16.6 ± 3.05 % and 52.5 ± 9.69 %, respectively, for PM<sub>2.5</sub>, in terms of the total fireworks. The quantification of the total, direct and indirect impacts of fireworks in the ambient PM gives a original contribution for understanding the physicochemical characteristics and mechanisms of such high-intensity anthropogenic activities.

## 1 Introduction

Atmospheric particulate matter (PM) is recognised globally as a major environmental issue with adverse effects on air quality, regional visibility, global climate change and health (Ding et al., 2008; Robichaud and Ménard, 2014). By scattering and absorbing incoming solar radiation and outgoing terrestrial radiation directly, or by acting as cloud-condensation nuclei and thereby influencing the optical properties of clouds indirectly, atmospheric aerosols can influence the radiation balance of the earth's atmosphere (Lin et al., 2013; Shen et al., 2013). Ambient PM is a complex mixture of components from a variety of sources, including those natural and anthropogenic (Zheng et al., 2005; Zhao et al., 2013a). In recent years, concerns about short-term air quality degradation events and their continuous negative effects on human health has increased, especially for PM pollution caused by high-intensity anthropogenic activities.

Firework displays are high-intensity anthropogenic activities that create notable air pollution and obvious short-term air-quality degradation. Firework displays are used to celebrate popular holidays, a practice common worldwide (e.g. at the New Year). During firework displays, there is usually a transient and spectacular increase in the PM pollution. Fireworks contain a variety of metal salts, such as chlorates and perchlorates (Wang et al., 2007; Crespo et al., 2012), leading to extremely high ambient concentrations of these species during celebrations. These heavy metals and perchlorates are all highly toxic (Shi et al., 2011) and are on average fine enough to be easily inhaled and present a health risk to susceptible individuals. Both the long-term and short-term hazardous impacts of fireworks on human health have been paid

significant attention by researchers (Wang et al., 2007; Vecchi et al., 2008; Crespo et al., 2012; Cheng et al., 2013).

Studies have demonstrated that the release of fireworks could be an important source category for atmospheric PM (Vecchi et al., 2008). Fireworks can influence the PM directly by emitting firework-related species (such as certain heavy metals). Additionally, the indirect effects, which are indirectly caused by the activities of firework displays, should be taken into consideration for firework events. For example, pyrotechnic device explosions can lead to resuspension of materials already deposited on the ground; biomass combustion (fireworks made from paper and an igniter) occurs when the fireworks are displayed and incinerated after display. Although firework-related pollution episodes are transient in nature, they are highly concentrated and their influence is continuous. Both the direct and indirect influences of fireworks might significantly contribute to PM and total annual metal emissions. However, the quantification of firework contributions, especially for its direct and indirect impacts, is very limited.

Studies on fireworks have mainly applied the following methods: burning fireworks in specific laboratories or fields to characterise their chemical properties (Tsai et al., 2012) and investigating the environmental impacts through ambient sampling during firework periods (Sarkar et al., 2010; Crespo et al., 2012). The former cannot reflect the actual ambient conditions and indirect impacts. For the latter, celebrations by fireworks are usually continued for only a few days. Thus, it has been very difficult to quantify the contributions of fireworks to ambient PM, especially for the quantification of indirect impacts. Selecting an appropriate period and site for this subject is key. Fireworks are more prevalent in certain places than others. China produces the most fireworks in the world (Shi et al., 2011). In addition, setting off fireworks is a traditional way to celebrate the Chinese New Year (CNY, Spring Festival) and is justifiably welcomed all over the country. CNY is the most important folk holiday in China. Celebrations during CNY season tend to spill over into the preceding and succeeding days (usually until the Lantern Festival, another important festival in China), along with sporadic fireworks. During the firework displays, the anthropogenic emission patterns are greatly changed (Huang et al., 2012). Many ordinary activities are decreased, such as certain industries and traffic (Feng et al., 2012), whereas degradation of the air quality may occur due to displays of fireworks. This provides a unique opportunity to study the drastic source changes and allows the quantification of the direct and indirect contributions of fireworks under significantly different emission patterns.

Therefore, the purpose of this work is to individually quantify the total, direct and indirect contributions of fireworks to size-resolved PM. A sampling campaign of PM<sub>10</sub> and PM<sub>2.5</sub> was performed before, during and after the CNY (as shown in Table S1 in the Supplement) in a megacity in China. The physicochemical characteristics of the PM during this folk

festival were investigated, and the influence of fireworks on the physicochemical changes was also studied. The tracer species of fireworks were discussed and then used for source identification. The total, direct and indirect contributions of fireworks to PM were modelled using positive matrix factorisation (PMF), peak analysis (PA) and chemical mass balance (CMB) models. The quantitative assessment of the fireworks' direct and indirect impacts on ambient PM gives an original contribution to understand physicochemical characteristics and mechanisms during firework displays. The findings will aid in studies on similar high-intensity anthropogenic activities.

## 2 Methodology

### 2.1 Sampling

The PM<sub>10</sub> and PM<sub>2.5</sub> samples were collected in Tianjin (a megacity in China). Tianjin, the largest harbour of northern China, is a fast-growing and economically developed city that has a population of more than 12 million and has more than 1.5 million automobiles. The air quality of Tianjin has declined with rapid urbanisation and industrialisation. The sampling site is on the rooftop of a six-story building that is located in a mixed residential and commercial area in Tianjin. Usually, substantial degradation would occur during the firework displays in such a mixed area. The map of the sampling site is indicated in Fig. S1 in the Supplement.

The sampling campaign of PM<sub>10</sub> and PM<sub>2.5</sub> was performed from 30 January 2013 to 24 February 2013, including periods before, during and after the CNY (until the Lantern Festival). The sampling periods and the corresponding Chinese lunar calendar were listed in Table S1. During the sampling periods, firework displays occurred for the celebration of the CNY holiday. For the period from the eve of CNY to the Lantern Festival, fireworks are allowed in China, and numerous fireworks are used; thus, this period is defined as a heavy-firework period. For the period before the eve of CNY, sporadic fireworks may be set off so it is defined as a light-firework period.

Based on our previous works and other related studies (Shi et al., 2009; Xue et al., 2010; Tian et al., 2013a; Zhao et al., 2013a, b), the PM<sub>2.5</sub> and PM<sub>10</sub> (24 h samples) were simultaneously collected on quartz-fibre filters and polypropylene-fibre filters using medium-volume air samplers (TH-150) at a flow rate of 100 L min<sup>-1</sup>. The detailed information for the sampling and quality assurance/quality control (QA/QC) are available in the Supplement.

### 2.2 Chemical analysis

The elemental compositions (Al, Si, Ca, V, Cr, Mn, Fe, Co, Cu, Zn, As and Pb) of the samples collected on the polypropylene-fibre filters were determined by inductively coupled plasma-mass spectrometry (ICP-AES) (IRIS

Intrepid II, Thermo Electron). Ion chromatography (DX-120, DIONEX) was used to analyse the water-soluble ions ( $\text{NO}_3^-$ ,  $\text{SO}_4^{2-}$ ,  $\text{Na}^+$ ,  $\text{K}^+$  and  $\text{Mg}^{2+}$ ) collected on the quartz-fibre filters. The organic carbon (OC) and elemental carbon (EC) concentrations of the samples on the quartz-fibre filters were determined by Desert Research Institute/Oregon Graduate Center (DRI/OGC) carbon analysis, a technique based on the Interagency Monitoring of Protected Visual Environments (IMPROVE) thermal/optical reflectance (TOR) protocol.

The background contamination was routinely monitored by blank tests. Enough blank tests were conducted and used to validate and correct the corresponding data. Certified reference materials (CRM, produced by National Research Center for Certified Reference Materials, China) were used for quality assurance and quality control. Blanks and duplicate sample analyses were performed for nearly 10 % of the samples. The pretreatment procedure, chemical analysis and QA/QC are described in detail in the Supplement and refer to our previous works and other related studies (Bi et al., 2007; Shi et al., 2009; Wu et al., 2009; Kong et al., 2010; Xue et al., 2010; Zhao et al., 2013a, b).

In addition, scanning electron microscopy (SEM) determinations were performed by a JEOL JSM-7500F equipped with an X-ray energy dispersive spectrometer (EDS) to perform a morphological characterisation and chemical analysis of the individual particles.

## 2.3 Modelling approaches

### 2.3.1 Receptor models

Two widely used receptor models, positive matrix factorisation (PMF) and chemical mass balance (CMB), were applied to quantify the total (sum of the direct and indirect contributions), direct and indirect contributions of fireworks.

PMF is a useful factorisation methodology that can identify potential source categories and source contributions when the source profiles are not known. It identifies the source profile matrix  $\mathbf{F}$  and quantifies the source contribution matrix  $\mathbf{G}$  based on observations at the receptor site ( $\mathbf{X}$ ). Following Paatro and Tapper (1994), the PMF model can be represented in matrix form as

$$\mathbf{X} = \mathbf{GF} + \mathbf{E}. \quad (1)$$

The elements of the source contribution matrix  $\mathbf{G}$  and source profile matrix  $\mathbf{F}$  are constrained to non-negative values for PMF. Positive matrix factorisation uses the residual matrix elements ( $e_{ik}$ ) and uncertainty estimates ( $\sigma_{ij}$ ) to calculate a minimum  $Q$  value by using a weighed least square method, which is defined as

$$Q(\mathbf{E}) = \sum_{i=1}^m \sum_{j=1}^n (e_{ij} / \sigma_{ij})^2, \quad (2)$$

where  $\sigma_{ij}$  is the uncertainty of the  $j$ th species in the  $i$ th sample, which is used to weight the observations that include

sampling errors, detection limits, missing data and outliers (Paatero, 2007). The goal of PMF is to minimise this function.

PM data from the different sizes ( $\text{PM}_{2.5}$  and  $\text{PM}_{10}$ ) were combined and inputted into PMF, as has been done in related works (Amato et al., 2009; Aldabe et al., 2011). The combined data showed satisfactory results, and further analysis demonstrated that the profiles of  $\text{PM}_{2.5}$  and  $\text{PM}_{10}$  were similar in this work. Additionally, different numbers of factors and different  $F_{\text{peak}}$  values were considered and tested when running PMF. The calculations were allowed to repeat 10 times from ten pseudorandom starting points for each computation to test if a global minimum point was reached. The error model code ( $\text{EM} = -14$ ) and the uncertainties required for PMF were chosen according to the user's guide (Paatero, 2007).

Then, the CMB model was applied to quantify the individual contributions from the direct and indirect impacts of fireworks. Chemical mass balance is also a widely used receptor model for cases in which the number and profiles of sources are available (Watson et al., 1984; Chen et al., 2012). Similar to PMF, the CMB can be described as

$$x_{ij} = \sum_{p=1}^p g_{ip} f_{pj} + e_{ij}, \quad (3)$$

where  $x_{ij}$  is the  $j$ th species concentration measured in the  $i$ th sample;  $f_{pj}$  is the  $j$ th species mass fraction in the  $p$ th source;  $g_{ip}$  is the contribution of the  $p$ th source to the  $i$ th sample; and  $e_{ij}$  is the residual (Hopke, 2003). In contrast to PMF, except for  $x_{ij}$ ,  $f_{pj}$  should also be available for the CMB model. The US EPA CMB8.2 (US EPA, 2004) was applied in this work. The main performance indices of CMB are the reduced chi square ( $\chi^2$ ), percent mass (PM) and  $R$  square ( $R^2$ ). Understanding the information of sources is important for the CMB modelling. In this work, a field survey of sources was performed before applying the CMB model to determine the source categories.

### 2.3.2 Peak analysis

In the present study, peak analysis was used to quantify the species abundances of the fireworks based on the observations of the PM and chemical species. This method was successfully applied to determine the profiles of the vehicle emissions (Ke et al., 2013). The highest and lowest PM or species concentrations were used to represent the peak and background observations, respectively. The peak period had the strongest fireworks density, whereas the background values corresponded to the lowest fireworks density. Then, the species abundances were obtained by normalising their concentrations with the corresponding PM concentrations, as follows (Ke et al., 2013):

$$F_j = \frac{c_{p,j} - c_{b,j}}{c_{p,\text{PM}}} - c_{b,\text{PM}}, \quad (4)$$

where  $F_j$  is the abundance (g per g of PM) for the  $j$ th species;  $C_{p,j}$  and  $C_{b,j}$  are the  $j$ th species concentrations ( $\mu\text{g m}^{-3}$ ) in the peak observation and the background observation, respectively;  $C_{p,\text{PM}}$  and  $C_{b,\text{PM}}$  are the PM concentrations ( $\mu\text{g m}^{-3}$ ) in the peak and the background observations, respectively.

The uncertainty ( $\sigma_{F_j}$ ) of the  $j$ th species abundance ( $F_j$ ) was defined as follows (Ke et al., 2013):

$$\sigma_{F_j} = F_j \sqrt{\left(\frac{\sigma_{p,j}}{C_{p,j}}\right)^2 + \left(\frac{\sigma_{b,j}}{C_{b,j}}\right)^2}, \quad (5)$$

where  $\sigma_{p,j}$  and  $\sigma_{b,j}$  are the measurement uncertainties ( $\mu\text{g m}^{-3}$ ) of the  $j$ th species in the peak observation and the background observation, respectively. The results of the peak analysis method were employed to describe the profiles of the total fireworks.

### 3 Results and discussion

#### 3.1 Physicochemical characteristics of PM<sub>10</sub> and PM<sub>2.5</sub>

The PM samples were acquired on two filters for each sampling day so consistency tests play an important role in the QA/QC process. The comparisons between the concentrations measured on the polypropylene-fibre filters and those on the quartz-fibre filters are shown in Fig. S2 in the Supplement. A satisfactory consistency (slopes close to unity and high correlations) was observed, indicating good quality assurance. Because the quartz-fibre filters tend to absorb water and become shredded during sample handling (Cheng et al., 2011), concentrations on the polypropylene-fibre filters were used in the following discussion.

The concentrations of the PM<sub>10</sub> and PM<sub>2.5</sub> in Tianjin during the sampling periods are summarised in Fig. S3 in the Supplement. The average concentration of PM<sub>10</sub> was  $212.95 \mu\text{g m}^{-3}$  and that of PM<sub>2.5</sub> was  $140.59 \mu\text{g m}^{-3}$ , with an average PM<sub>2.5</sub> / PM<sub>10</sub> ratio of 0.66. The PM<sub>2.5</sub> / PM<sub>10</sub> values were 0.65 and 0.66 during the light-firework and heavy-firework periods, respectively. The  $t$  test was used to analyse the difference between the PM<sub>2.5</sub> and PM<sub>10</sub> values in the two periods, and the results indicated an insignificant difference with  $p > 0.05$ . The PM<sub>10</sub> and PM<sub>2.5</sub> concentrations were  $148.74 \mu\text{g m}^{-3}$  and  $96.80 \mu\text{g m}^{-3}$ , respectively, during the light-firework period and  $249.08 \mu\text{g m}^{-3}$  and  $165.23 \mu\text{g m}^{-3}$ , respectively, during the heavy-firework period. The highest concentrations were observed on the eve of CNY, when massive firework displays usually occur all over the country (Feng et al., 2012), indicating the huge influence of fireworks on the PM concentrations. Additionally, the concentrations of PM<sub>10</sub> and PM<sub>2.5</sub> during non-firework period were  $133.30 \mu\text{g m}^{-3}$  and  $83.98 \mu\text{g m}^{-3}$ , which were sampled from Tianjin in March and April 2013. Compared with the non-firework period, the PM levels during light-firework period

were slightly higher and those during heavy-firework period were much higher.

The study of the chemical composition is critical for understanding the physicochemical characteristics of pollution during the folk festival. The average concentrations of the chemical species in PM<sub>10</sub> and PM<sub>2.5</sub> during the light-firework period and the heavy-firework period are exhibited in Fig. 1, and the abundance of the species (fractions of the species in PM) in PM<sub>10</sub> and PM<sub>2.5</sub> are summarised in Fig. S4 in the Supplement. According to Fig. 1 and Fig. S4 in the Supplement, the crustal elements (Al, Si, Fe and Ca), carbonaceous species (OC and EC) and several water-soluble ions ( $\text{Cl}^-$ ,  $\text{NO}_3^-$  and  $\text{SO}_4^{2-}$ ) were important species in PM<sub>10</sub> and PM<sub>2.5</sub> during the sampling periods. The concentrations of OC were  $9.84$  and  $15.58 \mu\text{g m}^{-3}$  for PM<sub>10</sub> and were  $7.61$  and  $11.32 \mu\text{g m}^{-3}$  for PM<sub>2.5</sub> during the light- and heavy-firework periods, respectively. The concentrations of EC were  $5.59$  (in PM<sub>10</sub> during the light-firework period),  $6.79$  (in PM<sub>10</sub> during the heavy-firework period),  $4.20$  (in PM<sub>2.5</sub> during the light-firework period) and  $4.55$  (in PM<sub>2.5</sub> during the heavy-firework period)  $\mu\text{g m}^{-3}$ . The ratio of OC / EC was higher during the heavy-firework period for both PM<sub>10</sub> and PM<sub>2.5</sub>, with values of  $1.76$  (light-firework) and  $2.32$  (heavy-firework) for PM<sub>10</sub> and  $1.81$  (light-firework) and  $2.49$  (heavy-firework) for PM<sub>2.5</sub>. Additionally, it was interesting to find that  $\text{K}^+$  played an important role during the heavy-firework period, in contrast to its effect during the light-firework period. Compared with prior studies (Kong et al., 2010; Tian et al., 2013b), several differences can be observed in chemical compositions.

In addition, for further characterisation, images and micrographs of the quartz-fibre filters are exhibited. Figure S5 in the Supplement shows photos of the quartz filters with the PM<sub>10</sub> and PM<sub>2.5</sub> samples for two cases: a normal day in the light-firework period and the eve of CNY in the heavy-firework period. A difference can be observed between the filters. Furthermore, Fig. S6 in the Supplement shows micrographs of PM<sub>2.5</sub> for the same days. There were many more particles for the samples from the eve of CNY than for those from the normal day, demonstrating the much higher concentration levels on the eve of CNY.

#### 3.2 Influence of fireworks on the physicochemical characteristics of PM pollution

Comparing the mass concentrations and abundances of species during the heavy-firework period with those during the light-firework period could help researchers learn more about the influence of this intensive human activity. As shown in Fig. 1, concentrations of most species (such as crustal elements, heavy metal species, carbonaceous species,  $\text{Cl}^-$ ,  $\text{Na}^+$ ,  $\text{K}^+$  and  $\text{Mg}^{2+}$ ) exhibited increasing trends during the heavy-firework period. It is believed that Al, Ca, Cr, Cu, Pb,  $\text{Cl}^-$ ,  $\text{Na}^+$ ,  $\text{K}^+$  and  $\text{Mg}^{2+}$  might represent firework-related species. Potassium is one of the major components

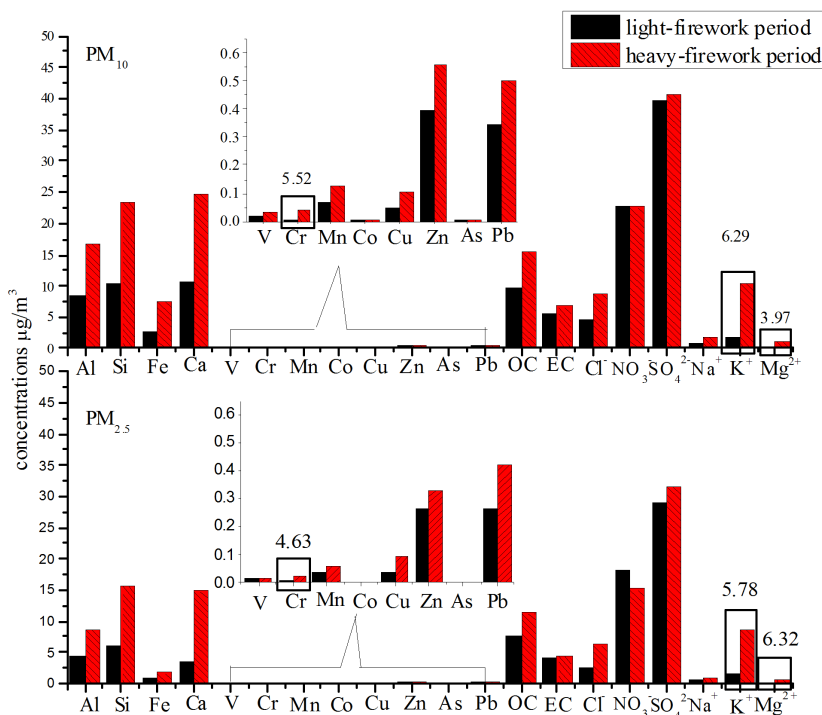


**Figure 1.** The averaged concentrations of the chemical species in PM<sub>10</sub> and PM<sub>2.5</sub> during the light-firework period and the heavy-firework period.

of fireworks because potassium compounds in black powder (commonly in the form perchlorate or chlorate) act as the main oxidisers during burning, with the corresponding chemical equations being  $2\text{KClO}_3 = 2\text{KCl} + 3\text{O}_2$  and  $\text{KClO}_4 = \text{KCl} + 2\text{O}_2$ . The Ca compounds (such as calcium chloride and sulfate) and Cu compounds (such as copper chloride and oxide) give rise to orange and blue colourations, respectively. A Cr compound ( $\text{CuCr}_2\text{O}_4$ ) is used as a catalyst for propellants. Cu, K, and Cr are used to provide silvery and glitter effects as well. Mg is a useful metallic fuel and is also used to produce sparks and crackling stars (in the form of the 50 : 50 Mg/Al alloy magnalium). Al also can be used alone as a common constituent for fuel, sparks and glitter effects. Pb can help to achieve steady and reproducible burning rates. Many components are in the form of perchlorate or chlorate, leading to high concentrations of  $\text{Cl}^-$ . The abruptly high emissions of these elements due to firework combustion can explain the high concentrations of these firework-related species in atmospheric PM during the heavy-firework period. It is noteworthy that certain firework-related heavy metals (Cr, Pb, Cu, etc.) are dangerous elements because of their toxicity and are forbidden by law in many countries. Such high concentrations in a short time, especially in a place where a considerable number of people are gathered, might be of concern.

Except for the directly firework-related species, an increase was also observed for most of the crustal elements

(such as Al, Si and Ca). Although Al and Ca might derive from industrial and direct firework sources, the abrupt increase of crustal elements might also be due to the resuspension of materials already deposited on the ground, caused by pyrotechnic device explosions. Additionally, higher concentrations of  $\text{K}^+$  and OC, which are good markers of biomass combustion, might imply the contribution of biomass combustion during the heavy-firework period. The higher concentrations of these indirect markers during the heavy-firework period can be ascribed partly to the indirect influence of fireworks. The important contributions of the resuspended dust and biomass combustion must be taken into consideration as sources of PM in these firework events. Moreover, the mass ratios of  $\text{NO}_3^-$  to  $\text{SO}_4^{2-}$  ( $\text{NO}_3^- / \text{SO}_4^{2-}$ ) during the heavy-firework period were lower than the ratios during the light-firework period. Similarly, lower  $\text{NO}_3^- / \text{SO}_4^{2-}$  during CNY was observed in Beijing (Feng et al., 2012). The change in  $\text{NO}_3^- / \text{SO}_4^{2-}$  might be partly due to differing formation mechanisms. Wang et al. (2007) reported the dominance of metal-catalysed heterogeneous formation of sulfate during the firework period. Goodman et al. (2001) reported a different formation mechanism for nitrate. However, the formation of secondary particles might be influenced by considerable factors (such as meteorological conditions and precursors) and is very complex.

Some of the species mentioned here require further study. SEM micrographs and EDS spectra of particles on the

normal day and on the eve of CNY are exhibited in Fig. S7 in the Supplement. The individual-particle analysis showed a higher K level on the eve of CNY than on the normal day. Furthermore,  $K^+$ , Cr and  $Mg^{2+}$  particularly stand out as species that have far higher concentrations during the heavy-firework period than during the light-firework period. The  $H/L$  values (the ratios of the concentrations in the heavy-firework period to those in the light-firework period) of the  $K^+$ , Cr and  $Mg^{2+}$  concentrations were 6.29, 5.52, 3.97 for  $PM_{10}$  and 5.78, 4.63, 6.32 for  $PM_{2.5}$  (as shown in Fig. 1), respectively. The mass concentrations may not completely reflect the composition of PM so a comparison of the species abundances was also performed. As shown in Fig. S4 in the Supplement, the abundances of  $K^+$ , Cr and  $Mg^{2+}$  were obviously higher during the heavy-firework period, with  $H/L$  values of 3.08, 4.44, 1.78 for  $PM_{10}$  and 2.68, 2.06 and 2.37 for  $PM_{2.5}$ , respectively. The high  $H/L$  values of the abundances can demonstrate the intensive influence of the fireworks on these species. For further investigation, the daily variations in the concentrations and abundances of the most firework-influenced species ( $K^+$ ,  $Mg^{2+}$  and Cr) are shown in Fig. S8 in the Supplement. Similar temporal patterns were observed for these species. Both the mass concentrations and abundances of  $K^+$ ,  $Mg^{2+}$  and Cr showed sharp peaks for the eve of CNY for  $PM_{2.5}$  and  $PM_{10}$ . Obvious increases also occurred on the fifth day of the Chinese lunar calendar and the Lantern Festival, which are important folk festival days for fireworks. Thus,  $K^+$ ,  $Mg^{2+}$  and Cr could indicate the influence of fireworks, which is important for further identification of the source categories of fireworks.

Species in PM may result from anthropogenic and natural sources. To focus the characteristics of anthropogenic emissions, the non-sea-salt (nss) ions were calculated. Assuming that all of the  $Na^+$  ions were from sea salt, the concentrations of nss  $SO_4^{2-}$ , nss  $Cl^-$ , nss  $K^+$  and nss  $Mg^{2+}$  in  $PM_{10}$  and  $PM_{2.5}$  were calculated based on the composition of average seawater. The relative mass concentrations of  $SO_4^{2-}$ ,  $Cl^-$ ,  $K^+$  and  $Mg^{2+}$  to  $Na^+$  are 0.252, 1.8, 0.037 and 0.119, respectively (Feng et al., 2012). Nearly all  $SO_4^{2-}$  and  $K^+$  (>98%) and most  $Mg^{2+}$  (>75%) ion in both  $PM_{10}$  and  $PM_{2.5}$  are from non-sea-salt. It is interesting to find a higher percentage of nss  $Cl^-$  in  $PM_{2.5}$  (72%) than in  $PM_{10}$  (57%), indicating the stronger influence of anthropogenic emissions on the  $Cl^-$  in fine PM. This result is reasonable because sea salt contributes a higher fraction to the coarse fraction of PM (Keuken et al., 2013). To investigate the anthropogenic impacts of fireworks, a comparison was conducted between nss ions during the light-firework and heavy-firework periods. The nss  $SO_4^{2-}$  accounts for more than 98% of the  $SO_4^{2-}$  in both the  $PM_{2.5}$  and  $PM_{10}$ , and there was no obvious difference ( $p > 0.05$ ) during the two periods. The concentrations of nss  $Cl^-$ , nss  $K^+$  and nss  $Mg^{2+}$  as well as their percentages in the total ions are exhibited in Fig. S9 in the Supplement. For these three ions, much higher concentrations and higher

percentages occurred during the heavy-firework period, especially on the eve of CNY, with more than 88% of the ions resulting from anthropogenic impacts. These results suggest the large anthropogenic influence on  $Cl^-$ ,  $K^+$ ,  $Mg^{2+}$ , which may be mainly caused by fireworks during the Chinese folk festival; as a result, they were effective to indicate the presence of fireworks. In the present work, the sources to  $Cl^-$  are complex, including not only anthropogenic but also natural sources (Vassura et al., 2014). Additionally, considering insufficient concentrations of Cr in the PM mass,  $K^+$  and  $Mg^{2+}$  may be more powerful as tracers of fireworks for the following source apportionment, as indicated by related reports (Wang et al., 2007; Cheng et al., 2013).

### 3.3 Sources of PM

To quantitatively evaluate the total, direct and indirect impacts of fireworks on ambient PM, source apportionment of size-resolved PM samples was modelled by the PMF, peak analysis and CMB models in this section.

#### 3.3.1 Total contributions of fireworks by PMF modelling

PMF was first applied to identify the possible source categories and to quantify their contributions to PM during the sampling periods. The variation in the  $Q$  values, actual conditions based on the field survey, the estimated source profiles and source contributions, the correlations between measured and estimated concentrations, were taken into consideration when judging the performance of PMF solutions. Finally, the five-factor solution and  $F_{\text{peak}} = 0.1$  were determined for fitting. The fitting plot between the measured and estimated PM concentrations is exhibited in Fig. S10 in the Supplement. The slope of the regression is 0.96, and the Pearson correlation coefficient is 0.98, suggesting perfect performance of PMF in this run (the estimated PM concentrations for most samples were similar to the measured concentrations).

The source profiles obtained by PMF are listed in Fig. 2 and Table S2 in the Supplement. According to Fig. 2, factor 1 exhibited high loadings for Al, Si, Ca, etc. (0.31, 0.35 and 0.63 in normalised source profiles as shown in Table S2 in the Supplement), which are associated with crustal dust (Pant and Harrison, 2012). In factor 2, relatively higher loadings of Al, Si and carbonaceous species were observed. Previous studies demonstrated that simultaneously high Al, Si and carbonaceous species might indicate coal combustion as the source category (Zhang et al., 2011; Pant and Harrison, 2012). Factor 3 correlates strongly with  $SO_4^{2-}$  and  $NO_3^-$ , consistent with source categories related to secondary particles (secondary sulfate and secondary nitrate) (Gao et al., 2011; Tian et al., 2013a). Factor 4 is mainly characterised by OC and EC (0.48 and 0.50 in normalised source profiles), which were indicative of vehicular exhaust (Pant

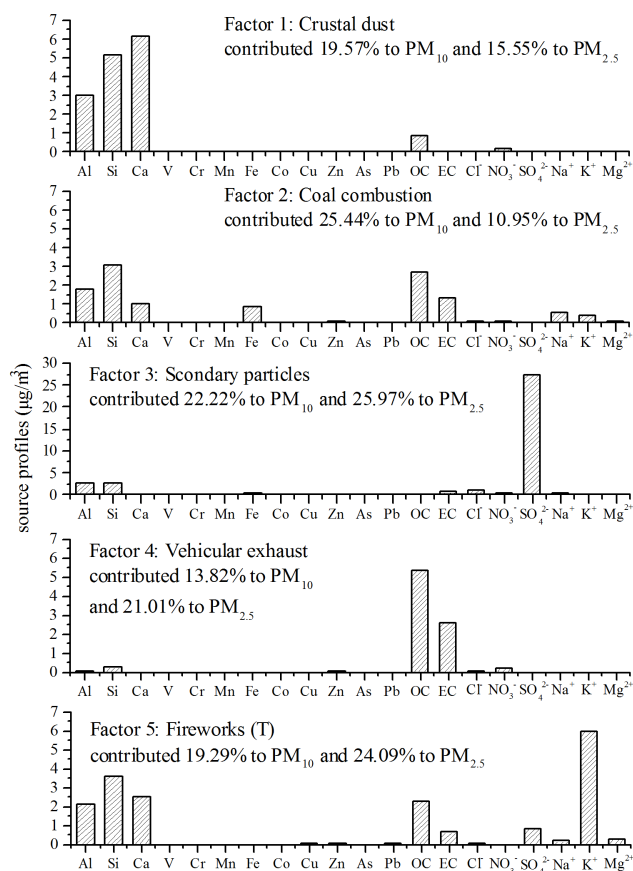


**Figure 2.** Source profiles ( $\mu\text{g m}^{-3}$ ) and percentage source contributions (%) estimated by PMF for  $\text{PM}_{10}$  and  $\text{PM}_{2.5}$ .

and Harrison, 2012). The percentage contributions of these source categories are summarised in Fig. 2 as well.

In factor 5,  $\text{K}^+$  presented obviously high weighting. As discussed above,  $\text{K}^+$  may be a tracer of fireworks. The higher loading of  $\text{Mg}^{2+}$  (0.65 in normalised source profiles in Table S2 in the Supplement) and Cr (0.71 in normalised source profiles) in this factor might also indicate the impacts of fireworks. Furthermore, it is interesting to find the relatively higher weighting of other species, such as OC, Al, Si and Ca. Strong links with  $\text{K}^+$  and OC could demonstrate biomass combustion (Cheng et al., 2013). Factor 5 was also associated with Al, Si and Ca, which are crustal elements. Biomass combustion might be indirectly caused by fireworks, which can occur when the fireworks are displayed and incinerated after display. Crustal elements might result from the resuspension of materials already deposited on the ground (caused by pyrotechnic device explosions). Therefore, factor 5 represented the total influence of fireworks, which might include the direct firework contribution and indirect impacts (biomass combustion and resuspended dust). Positive matrix factorisation extracts source profiles and quantifies contributions based on the temporal variation of the chemical species so source categories in one emission pattern might be identi-

fied as one factor. In this work, direct fireworks, resuspended dust and biomass combustion caused by fireworks may have similar emission patterns.

As exhibited in Fig. 2, the total influence of fireworks, including the direct firework and indirect impacts, contributed 19.29 % to  $\text{PM}_{10}$  and 24.09 % to  $\text{PM}_{2.5}$  during all sampling periods. The averaged percentage source contributions to  $\text{PM}_{10}$  and  $\text{PM}_{2.5}$  during the light-firework and heavy-firework periods, respectively, are calculated and shown in Fig. 3. A large difference can be observed. During the light-firework period, the total influence of fireworks contributed 4.28 % to  $\text{PM}_{10}$  and 7.18 % to  $\text{PM}_{2.5}$  while during the heavy-firework period, the total influence of the fireworks increased to rather high fractions (23.40 % for  $\text{PM}_{10}$  and 29.66 % for  $\text{PM}_{2.5}$ ). The time series of the percentage contributions of the total firework impacts on  $\text{PM}_{10}$  and  $\text{PM}_{2.5}$  are exhibited in Fig. 4, which could represent the trend of the total firework impacts (including direct fireworks, resuspended dust and biomass combustion). The most significant peak of the total firework contributions was presented on the eve of CNY, indicating the heavy impacts of the total fireworks on this day although the contributions may be overestimated due to the uncertainties in the results by PMF. In most cities in China, fireworks are allowed from the eve of CNY to the Lantern Festival (namely, the heavy-firework period in this work). Numerous fireworks were displayed on the eve of CNY, as it is the most important celebration of the year. Another peak of firework contributions was observed during the Lantern Festival. The Lantern Festival is also an important festival in China and is the last day that fireworks are allowed. The variation in the firework contributions was consistent with the Chinese folk celebrations, which demonstrate the good performance of PMF for modelling the total firework contributions in this work.

### 3.3.2 Species abundances of the total firework impacts

In addition to PMF, peak analysis was also employed to better understand the total firework impacts. As discussed above, the profiles and contributions of the total firework impacts were determined by PMF for  $\text{PM}_{10}$  and  $\text{PM}_{2.5}$ . Furthermore, peak analysis (Ke et al., 2013) was employed in this section to investigate the species abundances of the total fireworks in terms of the observations. The species abundances of the total firework impacts obtained by the two independent methods (PMF and peak analysis) are exhibited in Fig. 5. Considering the complexity mentioned previously, the secondary ions were not included in the comparison. Comparing the firework profiles, the abundances of most chemical species by peak analysis were similar to the corresponding values by PMF. As shown in Fig. 5, the abundance of  $\text{K}^+$ , which is the main marker of direct fireworks as discussed above, was consistent in the three firework profiles, with values of 16.34 % by PMF, 15.21 % by peak analysis for  $\text{PM}_{10}$  and 17.33 % by peak analysis for  $\text{PM}_{2.5}$ . The

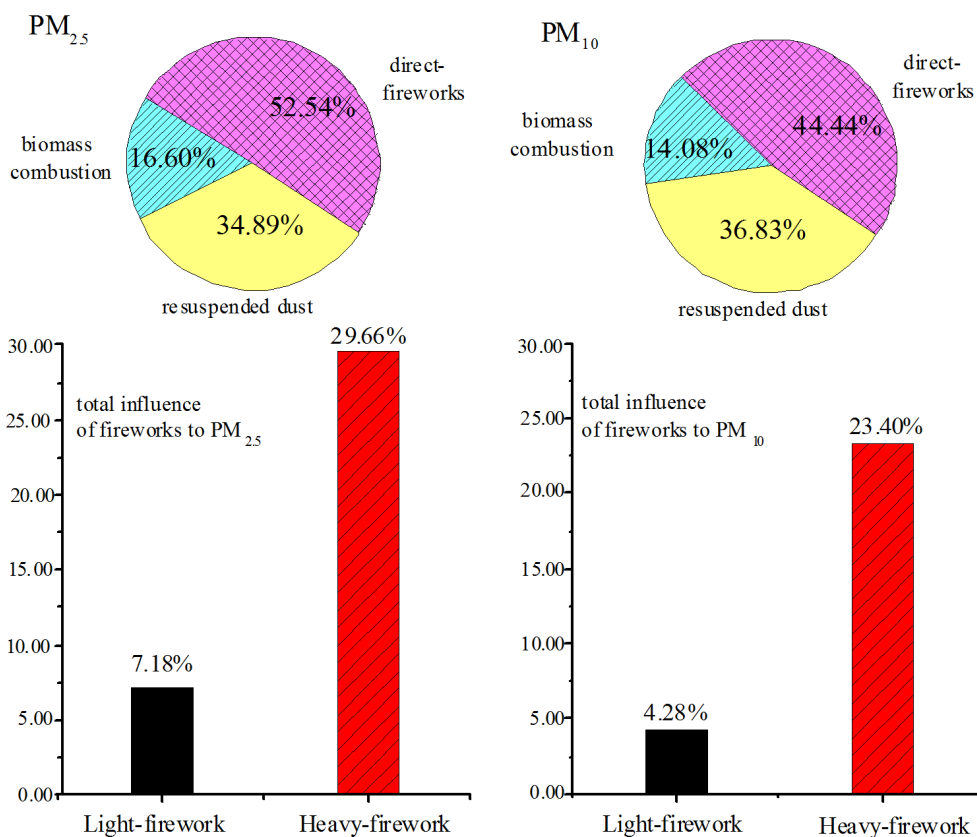


**Figure 3.** The total influence of fireworks on PM<sub>10</sub> and PM<sub>2.5</sub> (%) during the light-firework and heavy-firework periods, estimated by PMF (column chart), and the individual percentage contributions to the total firework impacts estimated by CMB based on peak analysis (pie chart).

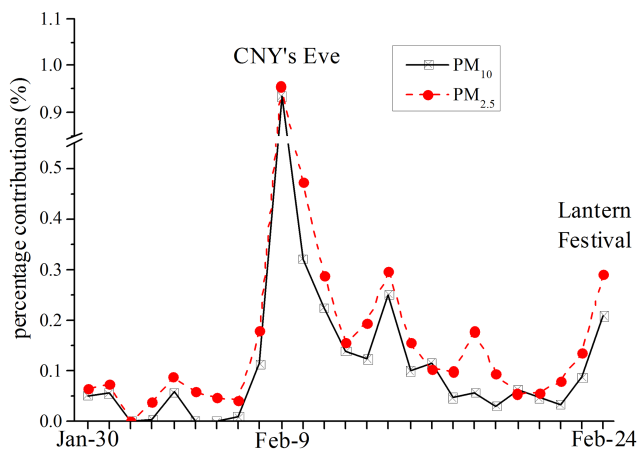


**Figure 4.** The daily percentage contributions of the total firework impacts to PM<sub>10</sub> and PM<sub>2.5</sub>, estimated by PMF.

Al, Si and Ca (resuspended dust elements) as well as OC (marker of biomass combustion along with K<sup>+</sup>) levels were also in agreement. The abundances of Al were 5.87, 6.72 and 7.02 %; Si were 9.87 %, 10.07 % and 11.85 %; and OC were

6.32, 5.87 and 6.60 %, estimated by PMF, by peak analysis for PM<sub>10</sub> and by peak analysis for PM<sub>2.5</sub>, respectively. For a further investigation of the similarity among these profiles, regression analyses and correlation coefficients (R) were computed and shown in Fig. 5. It is clear from Fig. 5 that all of the correlation coefficients were greater than 0.9, suggesting that the total firework profiles obtained by PMF and by peak analysis were concordant. In addition, the firework profiles of PM<sub>2.5</sub> were similar with those of PM<sub>10</sub>, implying that it is reasonable to introduce the combined data set of PM<sub>2.5</sub> and PM<sub>10</sub> into PMF.

### 3.3.3 Contributions of the direct and indirect firework impacts

As discussed above, the total influence of the fireworks might include indirect impacts (resuspended dust and biomass combustion) and direct fireworks. Thus, it is necessary to deeply evaluate the individual impacts of fireworks. In this work, the total firework profiles calculated by peak analysis were applied as the receptors in the CMB model, and the source profiles of three contributors (resuspended dust, biomass combustion and direct fireworks) were incorporated into the



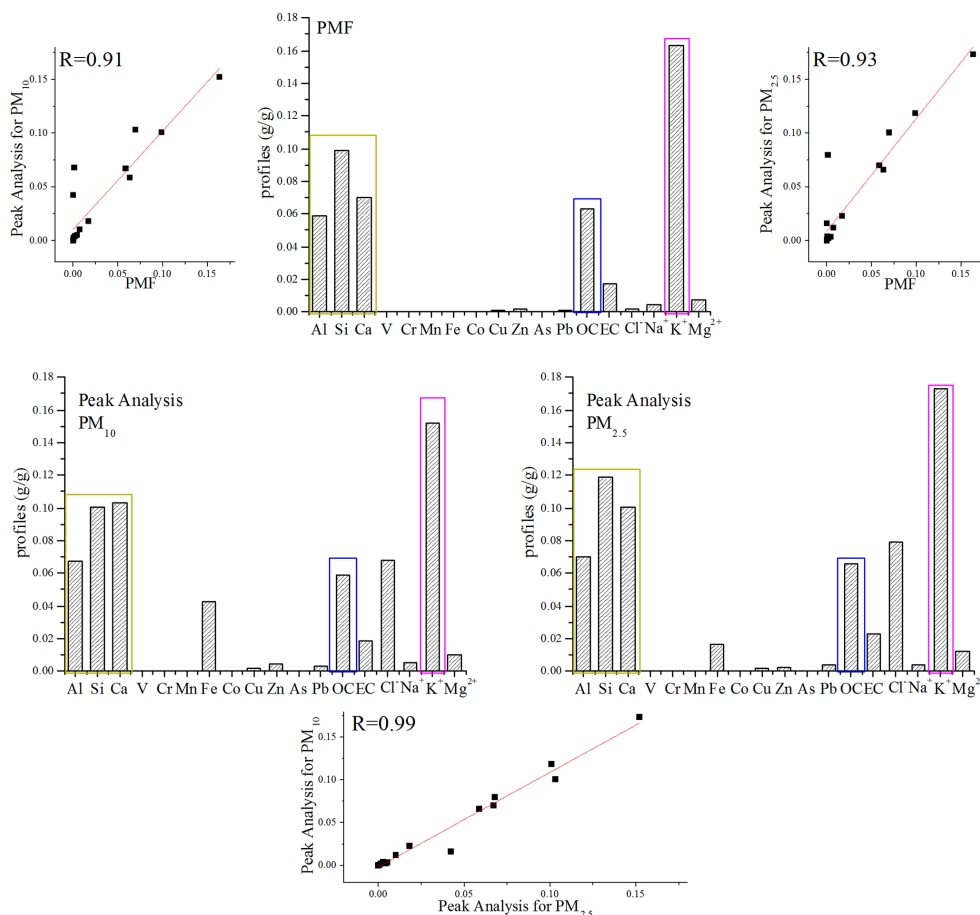


**Figure 5.** Profiles of fireworks (g/g) estimated by PMF for PM<sub>10</sub> and PM<sub>2.5</sub>, peak analysis for PM<sub>10</sub> and peak analysis for PM<sub>2.5</sub>, and the regression plots between these profiles.

model to individually determine the direct and indirect impacts of fireworks. In this work, the source profiles of the resuspended dust were from our prior works in Tianjin (Zhang et al., 2011); the biomass combustion profiles were from SPECIATE 4.0 of the US EPA; and the firework profiles were taken from a reported work (Tsai et al., 2012). The performance indices of CMB in this work were summarised in Table S3. The values of the performance indices met the requirements, indicating that the results of CMB might be reliable.

The individual contributions to the total firework impacts (based on peak analysis) are exhibited in Fig. 3 and Table S3 in the Supplement. According to the estimations, the percentage contributions of resuspended dust, biomass combustion and direct fireworks were  $36.82 \pm 8.37\%$ ,  $14.08 \pm 2.82\%$  and  $44.44 \pm 8.26\%$ , respectively, for PM<sub>10</sub>, accounting for the total firework contribution. For PM<sub>2.5</sub>, the percentage contributions were estimated to be  $34.89 \pm 4.19\%$  from resuspended dust,  $16.60 \pm 3.05\%$  from biomass combustion, and  $52.54 \pm 9.69\%$  from direct fireworks. The sum of resuspended dust, biomass burning and direct fireworks was

$> 100\%$  for PM<sub>2.5</sub> and  $< 100\%$  for PM<sub>10</sub>, however, they were in the range of 80–120%, which met the requirements of the CMB. The results demonstrated that fireworks can lead to a comprehensive influence on the ambient PM. In addition to the direct firework influence, resuspended dust and biomass combustion indirectly caused by fireworks should also be considered.

#### 4 Conclusions

To quantify the total, direct and indirect impacts of fireworks, size-resolved PM samples were collected in a megacity in China. The sampling campaign covered a Chinese folk festival (CNY), which provides a unique opportunity to quantify the contributions of fireworks under significantly different emission patterns. The strong influence of fireworks on the physicochemical characteristics of atmospheric PM<sub>10</sub> and PM<sub>2.5</sub> was observed. The highest PM concentrations were observed on the eve of CNY, when massive firework displays usually take place all over the country. The concentrations of most species (such as crustal elements, heavy metal species,

carbonaceous species,  $\text{Cl}^-$ ,  $\text{Na}^+$ ,  $\text{K}^+$  and  $\text{Mg}^{2+}$ ) exhibited increased trends during the heavy-firework period. Among these,  $\text{K}^+$ ,  $\text{Mg}^{2+}$  and Cr showed the most obvious increase, and the results of non-sea-salt ions demonstrated the anthropogenic influence on these species.  $\text{K}^+$ ,  $\text{Mg}^{2+}$  and Cr can be good tracers for fireworks, especially for  $\text{K}^+$  and  $\text{Mg}^{2+}$ , which had higher concentrations. Subsequently, source apportionment was conducted using receptor models. The total influence of fireworks was quantified by PMF, contributing higher fractions during the heavy-firework period than those during the light-firework period. The profiles of the total fireworks obtained by PMF and peak analysis were consistent, with higher abundances of  $\text{K}^+$ , Al, Si, Ca and OC. Finally, the individual contributions of the direct and indirect impacts of fireworks were determined by the CMB model based on profiles from peak analysis. The present study demonstrated that fireworks might lead to a comprehensive influence on the ambient PM. Both the direct influence and indirect impacts (resuspended dust and biomass combustion) caused by fireworks should be considered. The present work can be helpful in understanding the physicochemical characteristics and mechanisms of such high-intensity anthropogenic activities.

**The Supplement related to this article is available online at doi:10.5194/acp-14-9469-2014-supplement.**

*Acknowledgements.* This study is supported by the National Natural Science Foundation of China (21207070 and 41375132), Special Funds for Research on Public Welfare of the Ministry of Environmental Protection of China (201409003) and the Ph.D. Candidate Research Innovation Fund of Nankai University.

Edited by: K. Schaefer

## References

- Aldabe, J., Elustondo, D., Santamaría, C., Lasheras, E., Pandolfi, M., Alastuey, A., Querol, X., and Santamaría, J. M.: Chemical characterisation and source apportionment of  $\text{PM}_{2.5}$  and  $\text{PM}_{10}$  at rural, urban and traffic sites in Navarra (North of Spain), *Atmos. Res.*, 1, 191–205, 2011.
- Amato, F., Pandolfi, M., Escrig, A., Querol, X., Alastuey, A., Pey, J., Perez, N., and Hopke, P. K.: Quantifying road dust resuspension in urban environment by multilinear engine: a comparison with PMF2, *Atmos. Environ.*, 17, 2770–2780, 2009.
- Bi, X. H., Feng, Y. C., Wu, J. H., Wang, Y. Q., and Zhu, T.: Source apportionment of  $\text{PM}_{10}$  in six cities of northern China, *Atmos. Environ.*, 41, 903–912, 2007.
- Chen, L.-W. A., Watson, J. G., Chow, J. C., Green, M. C., Inouye, D., and Dick, K.: Wintertime particulate pollution episodes in an urban valley of the Western US: a case study, *Atmos. Chem. Phys.*, 12, 10051–10064, doi:10.5194/acp-12-10051-2012, 2012.
- Cheng, Y., Zou, S. C., Lee, S. C., Chow, J. C., Ho, K. F., Watson, J. G., Han, Y. M., Zhang, R. J., Zhang, F., Yau, P. S., Huang, Y., Bai, Y., and Wu, W. J.: Characteristics and source apportionment of  $\text{PM}_{10}$  emissions at a roadside station, *J. Hazard. Mater.*, 195, 82–91, 2011.
- Cheng, Y., Engling, G., He, K.-B., Duan, F.-K., Ma, Y.-L., Du, Z.-Y., Liu, J.-M., Zheng, M., and Weber, R. J.: Biomass burning contribution to Beijing aerosol, *Atmos. Chem. Phys.*, 13, 7765–7781, doi:10.5194/acp-13-7765-2013, 2013.
- Crespo, J., Yubero, E., Nicolás, J. F., Lucarelli, F., Nava, S., Chiari, M., Calzolari, G.: High-time resolution and size-segregated elemental composition in high-intensity pyrotechnic exposures, *J. Hazard. Mater.*, 241–242, 82–91, 2012.
- Ding, X., Zheng, M., Yu, L. P., Zhang, X. L., Weber, R. J., Yan, B., Russell, A. G., Edgerton, E. S., and Wang, X. M.: Spatial and Seasonal Trends in Biogenic Secondary Organic Aerosol Tracers and Water-Soluble Organic Carbon in the Southeastern United States, *Environ. Sci. Technol.*, 42, 5171–5176, 2008.
- Feng, J. L., Sun, P., Hu, X. L., Zhao, W., Wu, M. H., and Fu, J. M.: The chemical composition and sources of  $\text{PM}_{2.5}$  during the 2009 Chinese New Year's holiday in Shanghai, *Atmos. Res.*, 118, 435–444, 2012.
- Gao, X., Yang, L., Cheng, S., Gao, R., Zhou, Y., and Xue, L.: Semi-continuous measurement of water-soluble ions in  $\text{PM}_{2.5}$  in Jinan, China: temporal variations and source apportionments, *Atmos. Environ.*, 45, 6048–6056, 2011.
- Goodman, A. L., Bernard, E. T., and Grassian, V. H.: Spectroscopic study of nitric acid and water adsorption on oxide particles: enhanced nitric acid uptake kinetics in the presence of adsorbed water, *J. Phys. Chem. A*, 105, 6443–6457, 2001.
- Hopke, P. K.: Recent developments in receptor modeling, *J. Chemom.*, 17, 255–265, 2003.
- Huang, K., Zhuang, G., Lin, Y., Wang, Q., Fu, J. S., Zhang, R., Li, J., Deng, C., and Fu, Q.: Impact of anthropogenic emission on air quality over a megacity – revealed from an intensive atmospheric campaign during the Chinese Spring Festival, *Atmos. Chem. Phys.*, 12, 11631–11645, doi:10.5194/acp-12-11631-2012, 2012.
- Ke, H. H., Ondov, J. M., and Rogge, W. F.: Detailed emission profiles for on-road vehicles derived from ambient measurements during a windless traffic episode in Baltimore using a multi-model approach, *Atmos. Environ.*, 81, 280–287, 2013.
- Keuken, M. P., Moerman, M., Voogt, M., Blom, M., Weijers, E. P., Röckmann, T., and Dusek, U.: Source contributions to  $\text{PM}_{2.5}$  and  $\text{PM}_{10}$  at an urban background and a street location, *Atmos. Environ.*, 71, 26–35, 2013.
- Kong, S. F., Han, B., Bai, Z. P., Chen, L. Shi, J. W., and Xu, J. W.: Receptor modeling of  $\text{PM}_{2.5}$ ,  $\text{PM}_{10}$  and TSP in different seasons and long-range transport analysis at a coastal site of Tianjin, China, *Sci. Total Environ.*, 408, 4681–4694, 2010.
- Lin, Z. J., Tao, J., Chai, F. H., Fan, S. J., Yue, J. H., Zhu, L. H., Ho, K. F., and Zhang, R. J.: Impact of relative humidity and particles number size distribution on aerosol light extinction in the urban area of Guangzhou, *Atmos. Chem. Phys.*, 13, 1115–1128, doi:10.5194/acp-13-1115-2013, 2013.
- Paatero, P.: User's guide for positive matrix factorization programs PMF2 and PMF3, part 1–2: tutorial, 19–21, University of Helsinki, Helsinki, Finland, 2007.
- Paatero, P. and Tapper, U.: Positive Matrix Factorization: a non-negative factor model with optimal utilization of error estimates of data values, *Environmetrics*, 5, 111–126, 1994.

- Pant, P. and Harrison, R. M.: Critical review of receptor modelling for particulate matter: A case study of India, *Atmos. Environ.*, 49, 1–12, 2012.
- Robichaud, A. and Ménard, R.: Multi-year objective analyses of warm season ground-level ozone and PM<sub>2.5</sub> over North America using real-time observations and Canadian operational air quality models, *Atmos. Chem. Phys.*, 14, 1769–1800, doi:10.5194/acp-14-1769-2014, 2014.
- Sarkar, S., Khillare, P. S., Jyethi, D. S., Hasan, A., and Parween, M.: Chemical speciation of respirable suspended particulate matter during a major firework festival in India, *J. Hazard. Mater.*, 184, 321–330, 2010.
- Shen, G. F., Tao, S., Wei, S. Y., Chen, Y. C., Zhang, Y. Y., Shen, H. Z., Huang, Y., Zhu, D., Yuan, C. Y., Wang, H. C., Wang, Y. F., Pei, L. J., Liao, Y. L., Duan, Y. H., Wang, B., Wang, R., Lv, Y., Li, W., Wang, X. L., and Zheng, X. Y.: Field Measurement of Emission Factors of PM, EC, OC, Parent, Nitro, and Oxy- Polycyclic Aromatic Hydrocarbons for Residential Briquette, Coal Cake, and Wood in Rural Shanxi, China, *Environ. Sci. Technol.*, 47, 2998–3005, 2013.
- Shi, G. L., Feng, Y. C., Zeng, F., Li, X., Zhang, Y. F., and Wang, Y. Q.: Use of a Nonnegative Constrained Principal Component Regression Chemical Mass Balance Model to Study the Contributions of Nearly Collinear Sources, *Environ. Sci. Technol.*, 43, 8867–8873, 2009.
- Shi, Y. L., Zhang, N., Gao, J. M., Li, X., and Cai, Y. Q.: Effect of fireworks display on perchlorate in air aerosols during the Spring Festival, *Atmos. Environ.*, 45, 1323–1327, 2011.
- Tian, Y. Z., Shi, G. L., Han, S. Q., Zhang, Y. F., Feng, Y. C., Liu, G. R., Gao, L. J., Wu, J. H., and Zhu, T.: Vertical characteristics of levels and potential sources of water-soluble ions in PM<sub>10</sub> in a Chinese megacity, *Sci. Total Environ.*, 447, 1–9, 2013a.
- Tian, Y. Z., Xiao, Z. M., Han, B., Shi, G. L., Wang, W., Hao, H. Z., Li, X., Feng, Y. C., and Zhu, T.: Seasonal Study of Primary and Secondary Sources of Carbonaceous Species in PM<sub>10</sub> from Five Northern Chinese Cities, *Aerosol Air Qual. Res.*, 13, 148–161, 2013b.
- Tsai, H. H., Chien, L. H., Yuan, C. S., Lin, Y. C., Jen, Y. H., and Ie, I. R.: Influences of fireworks on chemical characteristics of atmospheric fine and coarse particles during Taiwan's Lantern Festival, *Atmos. Environ.*, 62, 256–264, 2012.
- US EPA (US Environmental Protection Agency): EPA-CMB8.2 Users Manual, US EPA, office of Air Quality Planning and Standards, Research Triangle Park, NC 27711, 2004.
- Vassura, I., Venturini, E., Marchetti, S., Piazzalunga, A., Bernardi, E., Fermo, P., and Passarini, F.: Markers and influence of open biomass burning on atmospheric particulate size and composition during a major bonfire event, *Atmos. Environ.*, 82, 21–225, 2014.
- Vecchi, R., Bernardoni, V., Cricchio, D., D'Alessandro, A., Fermo, P., Lucarelli, F., Nava, S., Piazzalunga, A., and Valli, G.: The impact of fireworks on airborne particles, *Atmos. Environ.*, 42, 1121–1132, 2008.
- Wang, Y., Zhuang, G. S., Xu, C., and An, Z. S.: The air pollution caused by the burning of fireworks during the lantern festival in Beijing, *Atmos. Environ.*, 41, 417–431, 2007.
- Watson, J. G., Cooper, J. A., and Huntzicker, J. J.: The effective variance weighting for least squares calculations applied to the mass balance receptor model, *Atmos. Environ.*, 18, 1347–1355, 1984.
- Wu, L., Feng, Y. C., Wu, J. H., Zhu, T., Bi, X. H., Han, B., Yang, W. H., and Yang, Z. Q.: Secondary organic carbon quantification and source apportionment of PM<sub>10</sub> in Kaifeng, China, *J. Environ. Sci.*, 21, 1353–1362, 2009.
- Xue, Y.H., Wu, J.H., Feng, Y.C., Dai, L., Bi, X.H., and Li, X.: Source Characterization and Apportionment of PM<sub>10</sub> in Panzhihua, China, *Aerosol Air Qual. Res.*, 10, 367–377, 2010.
- Zhang, Y. F., Xu, H., Tian, Y. Z., Shi, G. L., Zeng, F., Wu, J. H., Zhang, X. Y., Li, X., Zhu, T., and Feng, Y. C.: The study on vertical variability of PM<sub>10</sub> and the possible sources on a 220 m tower, in Tianjin, China, *Atmos. Environ.*, 45, 6133–6140, 2011.
- Zhao, P. S., Dong, F., He, D., Zhao, X. J., Zhang, X. L., Zhang, W. Z., Yao, Q., and Liu, H. Y.: Characteristics of concentrations and chemical compositions for PM<sub>2.5</sub> in the region of Beijing, Tianjin, and Hebei, China, *Atmos. Chem. Phys.*, 13, 4631–4644, doi:10.5194/acp-13-4631-2013, 2013a.
- Zhao, X. J., Zhao, P. S., Xu, Meng, W., Pu, W. W., Dong, F., He, D., and Shi, Q. F.: Analysis of a winter regional haze event and its formation mechanism in the North China Plain, *Atmos. Chem. Phys.*, 13, 5685–5696, doi:10.5194/acp-13-5685-2013, 2013b.
- Zheng, M., Salmon, L. G., Schauer, J. J., Zeng, L. M., Kiang, C. S., Zhang, Y. H., and Cass, G. R.: Seasonal trends in PM<sub>2.5</sub> source contributions in Beijing, China, *Atmos. Environ.*, 39, 3967–3976, 2005.